Bulletin of the Seismological Society of America, Vol. 108, No. 5A, pp. 2756–2763, October 2018, doi: 10.1785/0120180059

A Local Magnitude Scale for Slovakia, Central Europe

by Zuzana Chovanová and Jozef Kristek

Abstract In this study, we present a local magnitude scale for the territory of Slovakia. Until now, the Hutton and Boore (1987) scale was used for local magnitude estimation in Slovakia. We collected trace amplitudes of earthquakes recorded by the National Network of Seismic Stations (NNSS) from 2005 to 2016 with epicentral distances of up to 550 km and a period within the interval $\langle 0.1, 2.0 \rangle$ s. Using linear regression analysis, we determined the distance correction term n and the attenuation term K. We determined the constant C according to Richter's definition of magnitude and we determined station corrections for nine stations. Using the newly determined scale reduces error by up to 58% compared to the formula previously used. We compared the obtained attenuation curve with those of neighboring and worldwide regions.

Introduction

Local magnitude scales are widely used to measure the size of earthquakes with epicentral distances of up to 600 km. The first local magnitude scale was developed by Richter (1935) in the form

$$M_L = \log A(R) - \log A_0(R). \quad (1)$$

The scale was defined as the maximum trace amplitude A in millimeters of an earthquake recorded by a Wood–Anderson seismograph with magnification of 2800, natural period 0.8 s, and damping 0.8 compared with the amplitude A_0 of a reference event of zero magnitude at the same distance R in kilometers. Richter defined the zero magnitude event as an event recorded at an epicentral distance of 100 km with a maximum trace amplitude of 0.001 mm. Richter also introduced values of $\log A_0$ for distances of 20–600 km for the southern California region. These values could be different for other regions as the seismic signal could be attenuated differently along its path toward seismic stations.

At the moment, the Wood–Anderson response is only simulated by using an appropriate filter in which the maximum trace amplitude is measured in nanometers. Uhrhammer and Collins (1990) found that using the Wood–Anderson seismograph with a magnification of 2800 overestimates M_L, so they proposed using a lower value of 2080. In practice, the Wood–Anderson filter is designed to provide static magnification equal to 1 and the original static magnification of 2080 is accounted for in the appropriate constant. The International Association of Seismology and Physics of the Earth's Interior (IASPEI) working group on magnitudes (IASPEI, 2013) suggested using the local magnitude formula in the form

$$M_L = \log A - n \log R - KR - C - S, \quad (2)$$

in which A is the maximum amplitude in nanometers simulated on a Wood–Anderson seismograph with a static magnification of 1, R is the epicentral distance in kilometers, C is a constant, and S is the station correction to take account of local conditions. Following the notation used by Bakun and Joyner (1984), parameters n and K represent geometrical spreading and attenuation, respectively.

Each country or region should have its own formula or at least a suitable calibration of equation (2) is often required to consistently reflect the seismic attenuation behavior in tectonic environments that differ from southern California (e.g., Di Bona, 2016). Recently, several studies and articles focused on estimating a local magnitude formula for Italy (e.g., Bobbio *et al.*, 2009; Di Bona, 2016), for Turkey (Kılıç *et al.*, 2017), for the United Kingdom (Ottemöller and Sargeant, 2013), for New Zealand (Ristau *et al.*, 2016), for Slovenia (Bajc *et al.*, 2013), for Greece (Scordilis *et al.*, 2013), for the Ethiopian Plateau (Brazier *et al.*, 2008), for the Ethiopian rift (Keir *et al.*, 2006), and for the Korean Peninsula (Kim and Park, 2005). Furthermore, the parameters in equation (2) may not be only regionally dependent but also directionally dependent as shown by Lolli *et al.* (2015) for Italy. However, there are still regions without a specific formula due to either a lack of local data or analysis. Therefore, for regions with similar attenuative properties to those of southern California, IASPEI (2013) recommends using the following formula:

$$M_L = \log A + 1.11 \log R + 0.00189R - 2.09. \quad (3)$$

This in fact is the same as the Hutton and Boore (1987) formula but with an amplitude in mm.

The National Network of Seismic Stations (NNSS) is the most important Slovak infrastructure for seismic activity

Table 1
Specification of National Network of Seismic Stations (NNSS) Seismic Stations and SMOL Station Used for This Analysis

ISC Code	Name	Latitude (°N)	Longitude (°E)	Altitude (m)	Label	Type
ZST	Železná studnička	48.20	17.10	250	1	Broadband
CRVS	Červenica	48.90	21.46	476	2	Broadband
KECS	Kečovo	48.48	20.49	345	3	Short period
KOLS	Kolonické sedlo	48.93	22.27	460	4	Broadband
STHS	Stebnícka Huta	49.42	21.24	534	5	Short period
VYHS	Vyhne	48.49	18.84	450	6	Broadband
MODS	Modra	48.37	17.28	520	7	Broadband
LANS	Liptovská Anna	49.15	19.47	705	8	Short period
SMOL	Smolenice	48.51	17.43	400	9	Short period

ISC, International Seismological Centre.

monitoring. Until 2003, the NNSS was not able to locate every earthquake on the Slovak territory with macroseismic effects. Modernizing the network in 2005 changed this. The NNSS is currently composed of 13 stations, five of which are broadband and the rest of which are short period (Table 1). Table 1 also includes the SMOL station, a part of the local seismic network around the Jaslovské Bohunice Nuclear Power Plant. All the data are processed by the Earth Science Institute of the Slovak Academy of Sciences. The Seismic Handler software package (Stammler, 1993) is used as the main seismic waveform analysis tool and M_L is computed using the equation (3). The maximum trace amplitude A is measured as the arithmetic mean of the maximum (zero-to-peak) on both of the horizontal component signal. The final, "network local magnitude" is computed as an average of local magnitudes determined at each seismic station that recorded the event. Until now, there was no study devoted to determining a local magnitude formula for the Slovak territory. Therefore, we decided to estimate the coefficients n, K, and C in equation (2). To reduce the differences between local magnitudes computed for one event at different NNSS stations, we also decided to estimate station corrections S. We focused our study on estimating these parameters for all of Slovakia, and we did not consider any directional dependency.

Slovakia is a country with moderate seismicity (Cipciar *et al.*, 2016). Two significant earthquakes with epicenters in Slovakia occurred through centuries. In 1443, central Slovakia was hit by an earthquake $M_w \cong 5.7$. The earthquake completely destroyed the mining city of Banská Štiavnica and heavy damages were reported also from other adjacent cities. The earthquake was felt in Austria, Poland, and Czech Republic. The extent of damages and shaken area indicates that the earthquake had tectonic origin. In 1906, the western part of Slovakia near Dobrá Voda village was hit by earthquake with $M_w = 5.9$. The earthquake caused cracks in the ground as well as heavy damages in the Dobrá Voda village (Réthly, 1907). The macroseismic depth of the earthquake was 9 km and the shaken area of $30,000$ km^2 included parts of Austria, Hungary, and the Czech Republic.

Most of the territory of Slovakia belongs to the Western Carpathians. The present day structure of the Western Carpathians contains a number of different allochthonous tectonic units (Biely *et al.*, 1996), displaced during the Alpine orogeny. The European platform, mainly the Bohemian massif is characterized by crust thickness of around 34 km. The crust thickness in the eastern Alps ranges in the interval of 38–44 km and around 40 km over most of the territory. It is the eastern continuation of the significant Alpine Moho depression, which reaches even 50 km depths in its central part. The morphology of the Moho varies from 44 km depth in the north Carpathians area to 26–28 km at the southern contact with the Pannonian basin system. The most distinctive inhomogeneity is a local depression of the Moho course and significant crust thickening in the northeastern portion of the Slovak territory. The minimum crust thickness of around 30–26 km is found in the Pannonian back-arc area. The minimal crust thicknesses follow the deepest Neogene depocentres of the Pannonian basin system. More on the tectonics of the studied region can be found in Hók *et al.* (2016).

Data

The Seismic Handler software stores the amplitude, the period at which the amplitude was measured, and the epicentral distance in the so-called EVT files. The dataset used in the analysis consists of trace amplitudes of earthquakes, quarry blasts, and mining events recorded between 2005 and 2016. It contains only events recorded on at least two investigated seismic stations and at epicentral distances of up to 550 km (Fig. 1). Because of the shape of the state borders, some of the epicenters are located outside Slovakia.

The majority of the data originate from mining events. These are clustered at two localities (Silesia and Lubin) around 300–400 km from seismic stations (Fig. 1). However, we excluded these data from the study because they do not satisfy the condition of evenly distributed epicenters in the region of interest.

Although the records of quarry blasts were not spatially clustered the maximum epicentral distance was around 260 km as shown on the histogram in Figure 2. Moreover the waveforms of these events are different than those of earthquakes; therefore, we excluded them from the dataset as well.

Figure 3 shows the distribution of the data of the final dataset with distance. We use linear (Fig. 3a) and logarithmic (Fig. 3b) distance scales, because equation (2) has both linear and logarithmic distance dependence. We can see good coverage in the range of $\langle 10, 550 \rangle$ km. Most of the trace

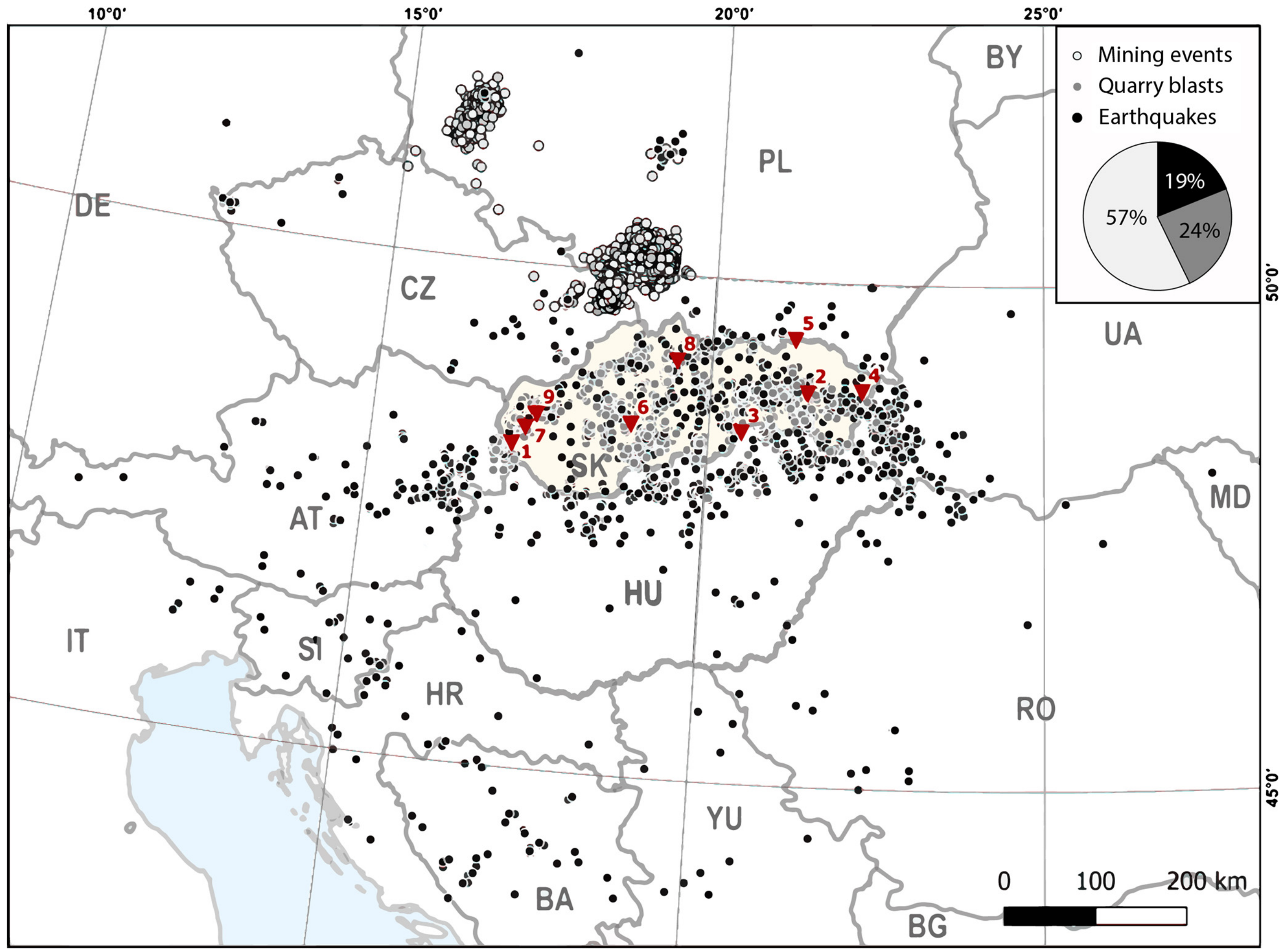

Figure 1. Primary dataset of the selected earthquakes, quarry blasts, and mining events used for the analysis recorded between 2005 and 2016. The dataset consists of events for which the local magnitude was computed at at least two seismic stations and with epicentral distances of up to 550 km. Seismic stations used for this analysis are indicated with numbered triangles and Slovakia is indicated by label SK. The color version of this figure is available only in the electronic edition.

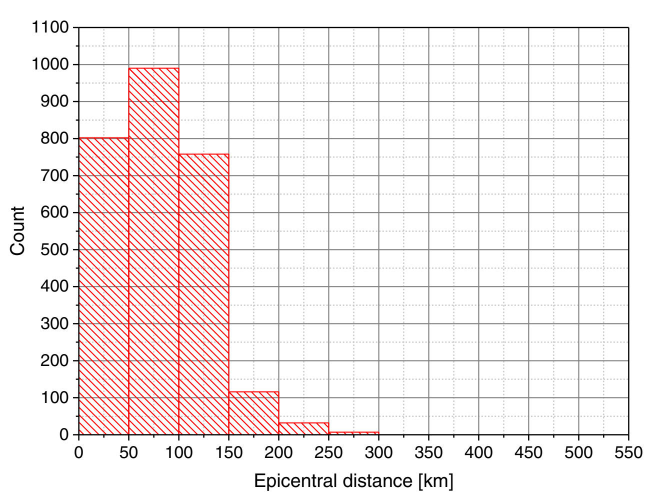

Figure 2. Histogram of trace amplitudes from primary dataset of trace amplitudes from quarry blast events. The color version of this figure is available only in the electronic edition.

amplitudes are from distances around 70–160 km. We also examined the periods of the observed trace amplitudes. We can see from the histogram in Figure 4 that the majority of the data lie within the interval $\langle 0.1, 2\rangle$ s and are sufficiently close to the natural period of the Wood–Anderson seismometer $T = 0.8$ s. Therefore, we kept in the final dataset only the data from this interval.

Method

Let N_E denotes the number of events and N_S is the number of stations. We can derive an overdetermined system of equations from equation (2) in the form:

$$\log A_{ji} = M_{\mathrm{L}j} + n \log R_{ji} + KR_{ji} + S_i + C;$$
$$j = 1, \ldots, N_E; \qquad i = 1, \ldots, N_S, \tag{4}$$

in which j indicates the jth event, i indicates the ith seismic station. Because not all the stations recorded the same event,

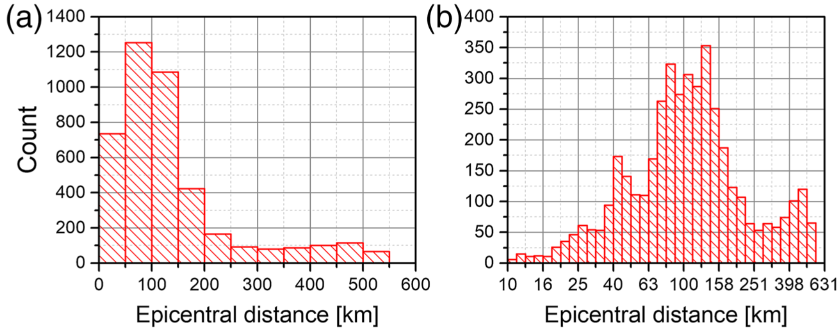

Figure 3. Histogram showing the distribution of trace amplitudes from final dataset with epicentral distance represented on (a) linear scale and on (b) logarithmic scale. The color version of this figure is available only in the electronic edition.

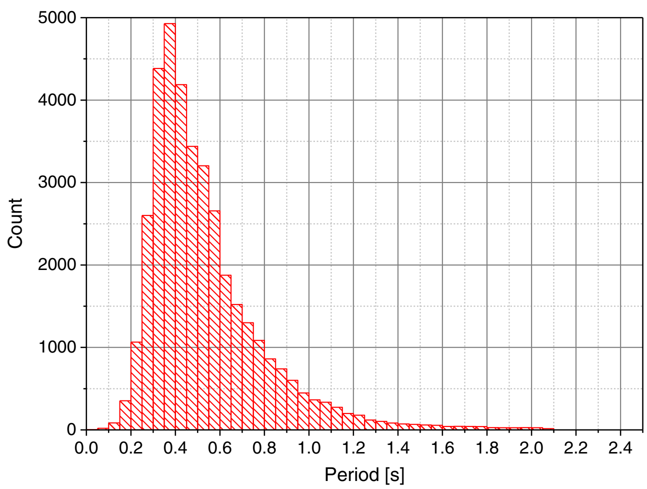

Figure 4. Histogram of periods of the dataset of trace amplitudes with epicentral distances within the interval of $\langle 10, 550 \rangle$ km. Most of the trace amplitudes are in the interval of $\langle 0.1, 2 \rangle$ s periods. The color version of this figure is available only in the electronic edition.

the total number of trace amplitudes A_{ji} is N. The local magnitude of the jth event $M_{\mathrm{L}j}$ and the constant C are coupled together and we cannot determine them separately. Therefore, we introduce M_j as

$$M_j = M_{\mathrm{L}j} + C, \tag{5}$$

and the system of equations (4) will be

$$\log A_{ji} = M_j + n \log R_{ji} + KR_{ji} + S_i; \quad j = 1, \ldots, N_E; \quad i = 1, \ldots, N_S. \tag{6}$$

The constant C along with station corrections will be specified in the last step according to Richter's definition of a magnitude. The station corrections satisfy the condition that the sum of all the station corrections is zero.

$$\sum_{i=1}^{N_S} S_i = 0. \tag{7}$$

The reason for such a condition is that for each earthquake we are interested in the "network local magnitude" computed as an arithmetic average of local magnitudes estimated from each station. Our aim is to reduce the variance in the values of local magnitudes for one earthquake recorded at multiple stations.

To solve equation (6), we have used the subroutine GELS from LAPACK95 (Barker *et al.*, 2001), which solves an overdetermined linear system with full rank matrix using **QR** factorization. **QR** factorization is also known as **QR** decomposition and is widely used to solve the linear least-squares problem. It is procedure of a decomposition of matrix **A** into a product of an orthogonal matrix **Q**, and an upper triangular matrix **R**.

Results

In the first step, we wanted to remove the outliers from the dataset. We solved the equation (6) for unknown parameters n, K, S_i and evaluated residuals r_{ji} as

$$r_{ji} = \log A_{ji} - (M_j + n \log R_{ji} + KR_{ji} + S_i); \quad j = 1, \ldots, N_E; \quad i = 1, \ldots, N_S. \tag{8}$$

Figure 5a shows the residuals together with their boxplot including the quartile and the outliers. Outliers were defined as the data outside the 1.5× interquartile range of residuals (IQR). After removing the outliers from the dataset, we repeatedly solved the equation (6) and removed the outliers until we obtained residuals without outliers. The final plot without outliers is in Figure 5b, in which we removed less than 6% of data identified as outliers.

In the next step, we searched for parameters n, K, and S_i which minimize the unbiased sample standard deviation of the residuals σ

$$\sigma = \sqrt{\frac{\sum r_{ji}^2}{N - (N_E + N_S + 1)}}. \tag{9}$$

This formula comes from losing one degree of freedom for each parameter estimated prior to estimating the standard deviation, which is in our case the sum of: N_E is the number of estimated magnitudes M_j, N_S is the number of estimated station corrections S_i, and 1 is the estimated mean residual (which equals 0 in this case) (see e.g., Chave, 2017). We have chosen the interval of values for seeking the parameter n $\langle -1.4, -0.7 \rangle$ based on the results of the first step of the analysis with the step 10^{-2} and for seeking the parameter K interval of values $\langle -0.004, -0.001 \rangle$ with the step

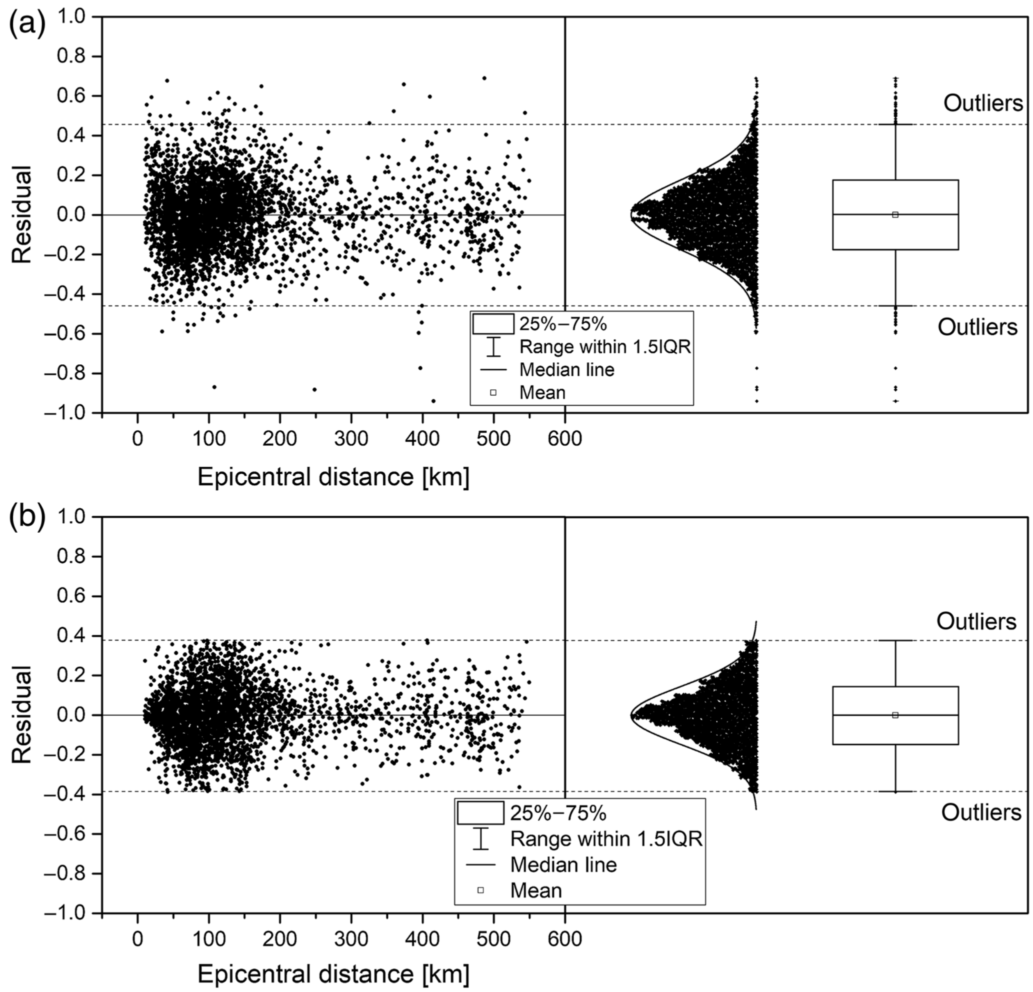

Figure 5. Residuals with boxplot showing quartile and outliers. Outliers were defined as data outside the 1.5× interquartile range of residuals (IQR). (a) Identified outliers from the first step of removal, and (b) residuals after last step of removal of the outliers.

4×10^{-5}. For each n and K from the intervals, we estimated M_j and S_i using regression analysis in the form:

$$\log A_{ji} - n \log R_{ji} - KR_{ji} = M_j + S_i, \quad (10)$$

to obtain the residuals equation (8). Knowing the residuals, we estimated σ using equation (9). Setting S_i as unknowns ensures the systematic errors at a particular station are separated from the residuals.

Figure 6 shows the unbiased sample standard deviation of residuals as a function of parameters n and K. The white star indicates the minimum value as $n = -1.05$, $K = -0.00236$. We clearly see the negative correlation between n and K. It is predictable as both are connected with an attenuation. The larger the geometrical spreading term is, the smaller the anelastic scattering attenuation should be, and vice versa.

In the next step, we determined the constant C according to Richter's definition of magnitude. Because we defined our formula for amplitudes in nanometers and the static magnification equals 1, the constant C is estimated as:

$$\begin{aligned} C &= M - \log A + n \times \log R + K \times R \\ &= 0 - \log \frac{1000}{2080} - 1.05 \log 100 - 0.00236 \times 100 \\ &\cong -2.02. \end{aligned} \quad (11)$$

The final developed M_L formula is

$$M_{Lj} = \log A_{ji} + 1.05 \log R_{ji} + 0.00236R_{ji} - 2.02. \quad (12)$$

Finally, we estimated station corrections for the nine seismic stations in Table 1 in the form

$$\log A_{ji} + 1.05 \log R_{ji} + 0.00236R_{ji} - 2.02 = M_{Lj} + S_i. \quad (13)$$

To compare the new formula with the formula of Hutton and Boore (1987) that has been used until now, we estimated an error E_i for each station i. We defined the error E_i as a sum of the absolute value of the mean of residuals r_{ji} and standard deviation for each station as:

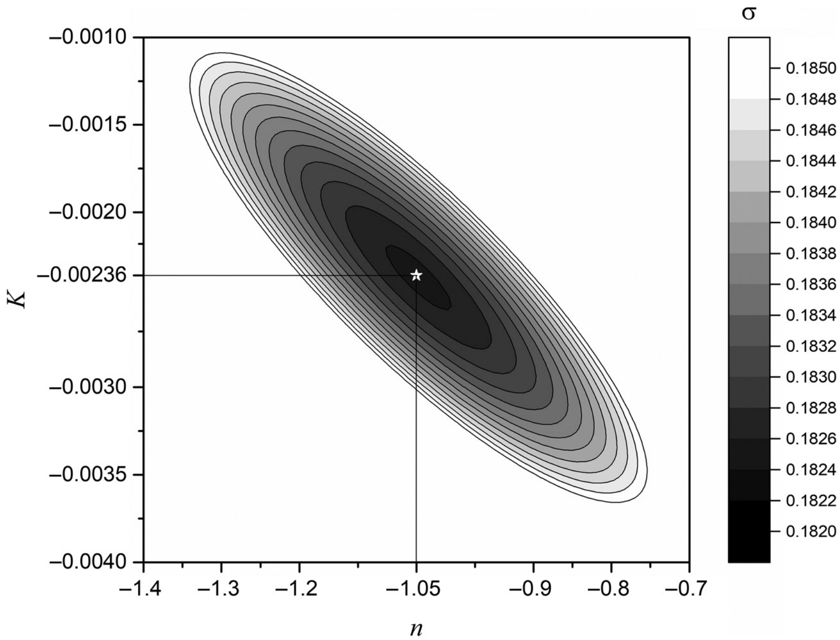

Figure 6. The unbiased sample standard deviation (σ) of residuals as a function of parameters n and K. The white star indicates the minimum.

$$E_i = \left| \frac{1}{N_E} \sum_{j=1}^{N_E} r_{ji} \right| + \sigma_i, \qquad \sigma_i = \sqrt{\frac{\sum_{j=1}^{N_E} r_{ji}^2}{N_E - 1}}. \tag{14}$$

This error quantifies the bias of the estimated local magnitudes from the network magnitudes at a specific station. In the case of a new scale, the first term (mean of residuals) equals zero because it takes into account the station corrections. In that case, the denominator of the σ_i in equation (14) should be N_E, but because $N_E \approx 1500$ and $N_E - 1$ make negligible difference, we can use the same formula and define the reduction of standard deviation as $1 - (E\ (\text{this study})/E(\text{IASPEI}))$. The results for all stations are compared in Table 2.

Discussion

First, we will look on meaning of the distribution of the data for the obtained results. The final formula is valid from 10–550 km. However, for short epicentral distances under 25 km, we can see (Fig. 3b) that for these epicentral distances we have less data and therefore estimated magnitudes could have larger bias. This should be taken into account when comparing with other studies. We should again note that the results may be affected by directional dependency, which we did not take into account. It is questionable if the amount of data is sufficient for such directional dependence analysis.

In following part, we will compare our findings to other studies. The newly developed M_L scale for Slovakia shows that the attenuation coefficients n and K do not change by more than 20% in comparison with coefficients of the Hutton and Boore (1987) scale that has been used so far. The attenuation curves ($-\log A_0$) for southern (SC) and central (CC) California, eastern North America (ENA), United Kingdom (UK), Hungary, Austria, and the curve obtained in this study (SK) are shown in Figure 7. The scales for Hungary and Austria are not published, they were provided by personal communication with Istvan Bodnar (2017) and Rita Meurers (2018). When comparing attenuation in the old (SC, Hutton and Boore, 1987) and the new (SK) curves, both are the same for distances of up to 100 km. However, beyond the distance of 100 km, the SC shows slightly lower attenuation. Bakun and Joyner (1984) show the same attenuation for the region of CC of up to 200 km, but for greater distances the SK attenuation is stronger. The SK curve is intermediate with respect to the regional scales of Hungary and Austria. Because the attenuation of Hungary is segmented with respect to distance, the ($-\log A_0$) compared to SK has slightly lower values for distances of $R \leq 50$ and $100 < R \leq 150$ km. Both the formulas used in Austria and the one defined by Kim (1998) for ENA do not include the attenuation K. This could lead to larger bias in larger epicentral distances. We see that they have the same slope of attenuation curves for epicentral distances larger than 300 km and both are shifted from others. The scale of Ottemöller and Sargeant (2013) shows that the attenuation of UK is intermediate between regions which are tectonically more active (CC, SC) and those which are more stable (e.g., Kim, 1998; ENA). The SK curve ($-\log A_0$) shows slightly higher attenuation for distances of $R \leq 150$ km than in the case of the UK curve.

Because there are no other works related to local magnitude attenuation for Slovakia, we can only compare

Table 2
Values of the Final Station Corrections and Errors of Estimating the Local Magnitude by the Formula Proposed in This Study and the One Previously Used

Station ISC Code	ZST	CRVS	KECS	KOLS	STHS	VYHS	MODS	LANS	SMOL
SC this study	0.06	0.03	−0.10	0.28	0.11	−0.21	0.03	−0.14	−0.06
Error of new scale	0.15	0.14	0.15	0.13	0.13	0.14	0.14	0.13	0.13
Error of old scale	0.25	0.19	0.22	0.31	0.21	0.27	0.21	0.19	0.17
Reduction of error	40%	26%	32%	58%	38%	48%	33%	32%	24%

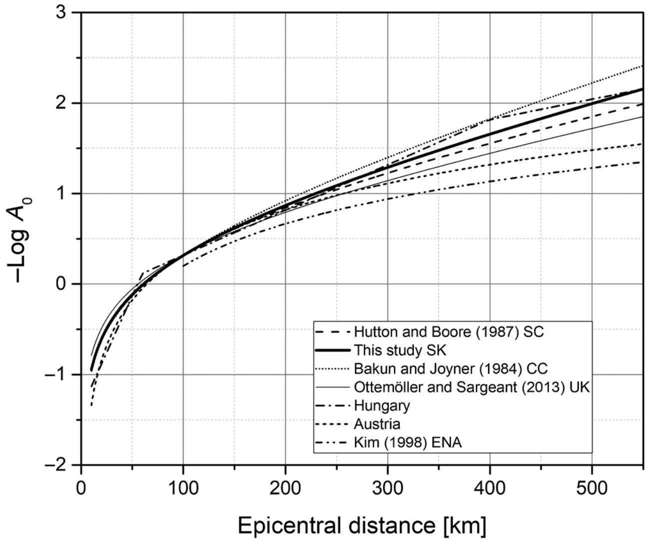

Figure 7. Comparison of attenuation curves for southern California (SC), central California (CC), Eastern North America (ENA), United Kingdom (UK), Hungary, Austria, and for the area of this study Slovakia (SK). Displacement amplitude is in nanometers.

macroseismic intensity attenuation curves. Labák (2000) showed that the macroseismic intensity attenuation curves for Western Carpathians have similar shapes as those for San Andreas Province in a sense that they fall in the same confidence interval. This is in a good agreement with our results if we compare our (SK) attenuation curve with SC and CC attenuation curves.

We computed station corrections and errors for nine seismic stations of the NNSS (Table 2). The station corrections are smaller than ±0.30. Applying the formula proposed in this study, the maximum error representing the bias of the estimated local magnitude at the specific station from the network magnitude is 0.15, whereas it is equal to 0.38 when the Hutton and Boore (1987) formula is used. The local magnitude formula proposed in this study allows us to reduce the error by up to 58%.

Because the differences between the newly developed scale and the previously used Hutton and Boore (1987) scale are not significant, the new scale will not significantly change the estimation of network local magnitudes. The main improvement of the newly developed scale is that the scatter of local magnitudes for one event will be significantly smaller thanks to the incorporation of station corrections.

Conclusions

We developed a new local magnitude scale for the territory of Slovakia, which we recommend to replace the Hutton and Boore (1987) scale that was previously used. This formula was obtained from a linear regression analysis of 3579 earthquake trace amplitudes recorded by nine seismic stations of the NNSS. The scale is valid from 10 to 550 km of epicentral distance. We inverted the attenuation parameters for the whole region of Slovakia, and we did not consider any directional dependency. The newly developed formula for the amplitude in nanometers and epicentral distance in kilometers is in the form $M_L = \log A + 1.05 \log R + 0.00236R - 2.02$. The $(-\log A_0)$ curve shows that the attenuation is intermediate compared to the regional scales of neighboring countries Hungary and Austria. The station corrections for the nine seismic stations of NNSS have been estimated for the first time. The reduction of error is up to 58% compared to the formula previously used. The improvement is mostly thanks to the incorporating station corrections in the new formula.

Data and Resources

Information about seismic stations has been taken from the website http://www.geo.sav.sk/en/structure-of-the-institute/laboratories/national-network-of-seismic-stations/ (last accessed February 2018). All data used in this article are from published sources listed in the references. The National Network of Seismic Stations (NNSS) data used in this study are available upon request. The graphics of distribution of different types of events used for the analysis is produced by EQUIS, spol. s. r. o.

Acknowledgments

This work has been supported by the Slovak Foundation Grant VEGA-2/0188/15. The authors would like to thank Costas Papazachos and Nikos Theodoulidis for the valuable discussions, Rita Meurers and Istvan Bondar for providing the local magnitude formulas, and all the colleagues who participate in the daily basis interpretation of the seismic data.

References

Bajc, J., Ž. Zaplotnik, M. Živčić, and M. Čarman (2013). Local magnitude scale in Slovenia, *Adv. Geosci.* **34,** 23–28.

Bakun, W. H., and W. B. Joyner (1984). The M_L scale in central California, *Bull. Seismol. Soc. Am.* **74,** 1827–1843.

Barker, V. A., L. S. Blackford, J. Dongarra, J. Du Croz, S. Hammarling, M. Marinova, and P. Yalamov (2001). *LAPACK95 Users' Guide*, SIAM, Philadelphia, Pennsylvania, 258 pp.

Biely, A., V. Bezák, M. Elečko, M. Kaličiak, V. Konečný, J. Lexa, J. Mello, J. Nemčok, M. Potfaj, and M. Rakús (1996). *Geological Map of Slovakia*, Ministry of Environment–Geological Survey of Slovak Republic, scale 1:500,000.

Bobbio, A., M. Vassallo, and G. Festa (2009). A local magnitude scale for southern Italy, *Bull. Seismol. Soc. Am.* **99,** 2461–2470.

Brazier, R., Q. Miao, A. Nyblade, A. Ayele, and C. Langston (2008). Local magnitude scale for the Ethiopian Plateau, *Bull. Seismol. Soc. Am.* **98,** 2341–2348.

Chave, A. D. (2017). *Computational Statistics in the Earth Sciences: With Applications in MATLAB*, Cambridge University Press, Cambridge, United Kingdom.

Cipciar, A., Z. Margočová, K. Csicsay, L. Fojtíková, E. Bystrický, M. Kristekova, P. Pažák, M. Galis, P. Franek, J. Kristek, *et al.* (2016). *Slovak Earthquake CatalogueVersion 2015*, Earth Science Institute, Slovak Academy of Sciences, Bratislava, Slovakia.

Di Bona, M. (2016). A local magnitude scale for crustal earthquakes in Italy, *Bull. Seismol. Soc. Am.* **106,** 242–258.

Hók, J., R. Kysel, M. Kovác, P. Moczo, J. Kristek, M. Kristeková, and M. Sujan (2016). A seismic source zone model for the seismic hazard assessment of Slovakia, *Geol. Carpath.* **67,** 275.

Hutton, L., and D. M. Boore (1987). The M_L scale in southern California, *Bull. Seismol. Soc. Am.* **77,** 2074–2094.

International Association of Seismology and Physics of the Earth's Interior (IASPEI) (2013). *Summary of Magnitude Working Group Recommendations on Standard Procedures for Determining Earthquake Magnitudes from Digital Data*, available at http://www.iaspei.org/commissions/commission-on-seismological-observation-and-interpretation (last accessed April 2018).

Keir, D., G. Stuart, A. Jackson, and A. Ayele (2006). Local earthquake magnitude scale and seismicity rate for the Ethiopian rift, *Bull. Seismol. Soc. Am.* **96,** 2221–2230.

Kılıç, T., L. Ottemöller, J. Havskov, K. Yanık, Ö. Kılıçarslan, F. Alver, and M. Özyazıcıoğlu (2017). Local magnitude scale for earthquakes in Turkey, *J. Seismol.* **21,** 35–46.

Kim, S. K., and M. A. Park (2005). The local magnitude scale in the Korean Peninsula, *Pure Appl. Geophys.* **162,** 875–889.

Kim, W.-Y. (1998). The M_L scale in eastern North America, *Bull. Seismol. Soc. Am.* **88,** 935–951.

Labák, P. (2000). Pravdepodobnostný výpočet charakteristík seizmického ohrozenia pre lokalitu atómových elektrární Bohunice, *Manuskript–dizertačná práca*, GFÚ SAV, Bratislava, Slovakia, 120 pp. (in Slovak).

Lolli, B., P. Gasperini, F. M. Mele, and G. Vannucci (2015). Recalibration of the distance correction term for local magnitude (M_L) computations in Italy, *Seismol. Res. Lett.* **86,** 1383–1392.

Ottemöller, L., and S. Sargeant (2013). A local magnitude scale M_L for the United Kingdom, *Bull. Seismol. Soc. Am.* **103,** 2884–2893.

Réthly, A. (1907). Earthquakes in Hungary in 1906, in *A m. kir. Orsz.*, Meteorológiai és Földmágnességi Intézet, Budapest, Hungary (in Hungarian).

Richter, C. F. (1935). An instrumental earthquake magnitude scale, *Bull. Seismol. Soc. Am.* **25,** 1–32.

Ristau, J., D. Harte, and J. Salichon (2016). A revised local magnitude (M_L) scale for New Zealand earthquakes, *Bull. Seismol. Soc. Am.* **106,** 398–407.

Scordilis, E., D. Kementzetzidou, and B. Papazachos (2013). Local magnitude estimation in Greece, based on recordings of the Hellenic unified seismic network (HUSN), *Bull. Geol. Soc. Greece* **47,** 1241–1250.

Stammler, K. (1993). SeismicHandler—Programmable multichannel data handler for interactive and automatic processing of seismological analyses, *Comput. Geosci.* **19,** 135–140.

Uhrhammer, R. A., and E. R. Collins (1990). Synthesis of Wood–Anderson seismograms from broadband digital records, *Bull. Seismol. Soc. Am.* **80,** 702–716.

Earth Science Institute
Slovak Academy of Sciences
Dúbravská cesta 9
84005 Bratislava, Slovakia
zuzana.margocova@savba.sk
(Z.C.)

Faculty of Mathematics, Physics and Informatics
Comenius University in Bratislava
Mlynská dolina F1
84248 Bratislava, Slovakia
kristek@fmph.uniba.sk
(J.K.)

Manuscript received 19 February 2018;
Published Online 4 September 2018